Thrust Generation in Electrostatic-Magnetic-Hybrid Plasma Thruster

IEPC-2019-A385

Presented at the 36th International Electric Propulsion Conference
University of Vienna • Vienna, Austria
September 15-20, 2019

D. Ichihara[1], T. Kato[2], A. Iwakawa[3], and A. Sasoh[4]
Department of Aerospace Engineering, Nagoya University, Nagoya, Aichi, 464-8603, Japan

Abstract: In this study, we developed two types of diverging magnetic field electrostatic thrusters that have a diverging magnetic field between a ring anode and a coaxially set hollow cathode. Two thrusters showed similar thrust characteristics that the obtained thrust were well fit to both the electrostatic thrust and electromagnetic thrust regardless of operating conditions. Calculated thrust coefficients for the electrostatic thrust and electromagnetic thrust were comparable. These tendencies indicate that both electrostatic and electromagnetic plasma accelerations contribute to generating thrust, namely the electrostatic-magnetic hybrid thrust generation was demonstrated. Because of the hybrid plasma acceleration method, thrust density reached 50 N/m^2, which is comparable or even higher with respect to conventional electrostatic thrusters.

Nomenclature

c, α, α'	=	coefficient
B	=	magnetic field strength
e	=	elementary charge
F	=	thrust
J_d	=	discharge current
J_k	=	keeper current
m_i	=	ion mass
$\dot{m}_a$	=	anode mass flow rate
$\dot{m}_c$	=	cathode mass flow rate
R	=	anode inner radius
V_d	=	discharge voltage

Subscripts

EM	=	electromagnetic
ES	=	electrostatic

I. Introduction

Electric propulsion is one of the external combustion engine that converting an electric energy to a kinetic energy. In an electrostatic acceleration thruster, injected propellant is ionized and accelerating only ions by using an electric potential difference between an anode and cathode. The most practicable electric propulsions such as ion engines and Hall thrusters are categorized in the electrostatic thruster. Because the electrostatic acceleration is a

[1] Research associate, Department of Aerospace Engineering, daisuke.ichihara@mae.nagoya-u.ac.jp.
[2] Graduate Student, Department of Aerospace Engineering, kato@fuji.nuae.nagoya-u.ac.jp.
[3] Lecturer, Department of Aerospace Engineering, iwakawa@nuae.nagoya-u.ac.jp.
[4] Professor, Department of Aerospace Engineering, akihiro.sasoh@mae.nagoya-u.ac.jp.

collision-less process, these thrusters achieve more than 60% of thrust efficiency with small discharge current (10^0 A) × high discharge voltage (10^2 V, much higher than the propellant ionization energy). Although the thrust is proportional to propellant flow rate, the thrust density has a physical[1] or practical[2] limitations. On the other hand, an electromagnetic thruster accelerate both ions and electrons at the same time by Lorentz force. In order to generate a large thrust, the thruster operation condition requires a large current (10^2 - 10^3 A) × small discharge voltage (10^1 V). Under this operating condition, the Lorentz force act on the electrons. While ions obtain momenta through the momentum exchange collisions with the electrons. Because of this collisional plasma acceleration process, the electromagnetic acceleration has no limitation for thrust density. However, thrust efficiency is typically less than 30% [3] due to the energy losses through the collisions.

In order toe realize the thruster that has high thrust efficiency with high thrust density, we have studied an electrostatic-magnetic hybrid plasma acceleration. In the electrostatic ion acceleration, ion's kinetic energy depends on the electric potential where the ion was generated. In electromagnetic acceleration, the momentum exchange collisions with electrons and diversion along the magnetic lines of force are important for increasing ion energy. In this study, we present two types of thrusters and those thrust characteristics about electrostatic-magnetic hybrid plasma acceleration.

II. Experimental Apparatus

In this section, thruster heads and thrust measurement apparatuses are described. Because the details of each thruster head and measurement system are described in our previous article[4], here we note the features of each equipment briefly.

A. Thruster Heads

1. Central Cathode Electrostatic Thruster 1

Figure 1 shows the schematic of the central cathode electrostatic thruster type 1 (CC-EST-1). The diverging magnetic field was applied by a water-cooled solenoid coil. By changing the coil current, the magnetic field at the center of the solenoid coil was varied from 100 mT to 250 mT. A ring anode had a 80-mm of inner diameter and 8 mm of an effective length. Inside the ring anode, a ceramic plate was installed to form a 1.5-mm-width slit to supply the propellant. A hollow cathode (Kaufmann & Robinson Inc., LHC–03–AE1–01, 20 A maximum) was coaxially located inside the ceramic plate. The exit plane of the hollow cathode was flash mounted to the ceramic plate.

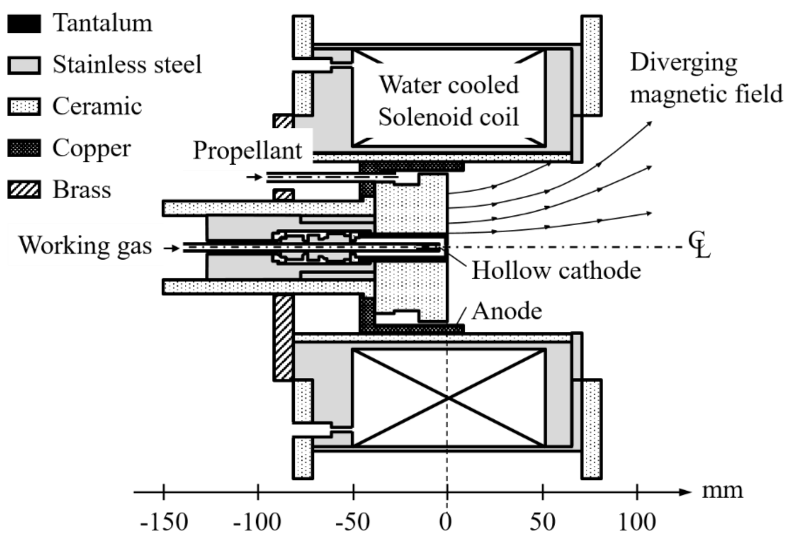

Figure 1 Schematic of the central cathode electrostatic thruster 1 (CC-EST-1)[4]

2. Central Cathode Electrostatic Thruster 2

Figure 2 shows the schematic of the central cathode electrostatic thruster type 2 (CC-EST-2). As well as the CC-EST-1, CC-EST-2 had the 1.5-mm-slit between the ring anode and the ceramic plate. The ring anode had a 30 mm of inner diameter and a 8 mm of an effective length. The same hollow cathode used in CC-EST-1was set on the center axis. Instead of the solenoid coil, a permanent magnet was used to apply the diverging magnetic field. By changing the material/size of the permanent magnet, magnetic field strength at the center of the magnet was varied from 210 mT to 402 mT.

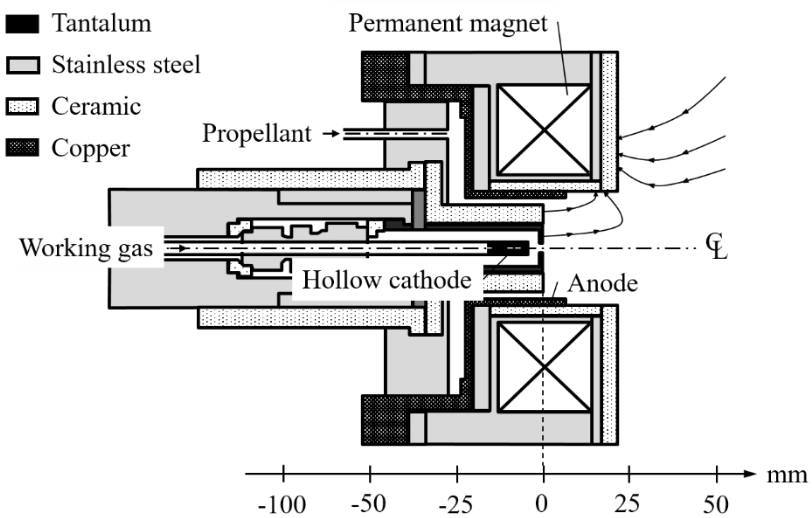

Figure 2   Schematic of the central cathode electrostatic thruster 2 (CC-EST-2)[4]

B. Gravity Pendulums for Thrust Measurement

Gravity pendulum type thrust stands with different types of fulcrums were used to directly measure the thrust. For CC-EST-1, the fulcrum was supported by a vacuum bellows[5] and for CC-EST-2, the fulcrum point was supported by two knife-edges[6]. The calibrated conversion factors were 259 ± 3.2 mN/V for the bellows pendulum, and 174 ± 0.33 mN/V for the knife-edge pendulum. Both thrust stand showed the same resolution of 0.2 mN, which was less than 3% of the minimum thrust value. The tare force was measured beforehand and was taken into account in the correction of thrust measurement.

III. Experimental Results and Discussions

A. Operating Conditions

Table 1 summarizes the investigated operating conditions. Propellant gas was xenon and its purity was 99.995%. The uncertainties in $\dot{m}_a$, V_d, and J_d were ± 10^{-2} mg/s, ± 2.0 V, and ± 51 mA, respectively. All experiments were conducted in a stainless-steel vacuum chamber. Under the operating conditions, background pressure was maintained in low-to-middle 10^{-2} Pa range.

Table 1   Thruster operating conditions.

Parameter	Unit	CC-EST-1	CC-EST-2
$\dot{m}_a$	mg/s	0.68 - 2.05	068 - 4.77
$\dot{m}_c$	mg/s	0.49	0.49
V_d	V	80 - 250	100 - 300
B	mT	100 - 250	210 - 402
J_k	A	2.0	2.0

B. Thrust Characteristics

The experimentally obtained thrust should have contributions from the electrostatic and/or electromagnetic accelerations. As is described in detail in Ref.4, the characteristic thrust for electrostatic acceleration is given by $\dot{m}_a(2eV_d/m_i)^{½}$ and for electromagnetic acceleration by J_dBR. The electrostatic thrust is expressed by

$$F = \alpha' \dot{m}_a \sqrt{2eV_d/m_i} \ . \qquad (1)$$

In an ideal electrostatic acceleration for singly charged ions, α' is unity. While if the obtained thrust was generated by an electrostatic-magnetic hybrid acceleration, F should be expressed also using J_dBR. Sasoh et al.[4] formulated the thrust generated by this type of plasma acceleration in a diverging magnetic field.

$$F = \alpha J_d BR \qquad (2)$$

$$\alpha \equiv \alpha_{ES} + \alpha_{EM} \ , \qquad (3)$$

where α_{ES} and α_{EM} are the thrust coefficients in electrostatic and electromagnetic acceleration, respectively. Due to the independency of electrostatic acceleration on the applied magnetic field, parameters α and α_{EM} are also related as

$$\alpha = c/B + \alpha_{EM} \ . \qquad (4)$$

The calculated α at each B was fitted to Eq. (4) by using a least-squares method, and α_{EM} was estimated as a fitting parameter. $\alpha_{ES} = c/B$ was calculated by subtracting α_{EM} from α.

Figure 3(a) shows the $\dot{m}_a(2eV_d/m_i)^{½}$ dependence of F with different thruster types. Regardless of the thruster types, obtained thrust was well fit by Eq. (1). The calculated α' were 0.7 in both thrusters. Because of ion energy loss and beam diverging loss, experimentally fitted α' was less than unity. Figure 3(b) shows the J_dBR dependence of F with different thrusters. In both thrusters, obtained F were well fitted with Eq. (2).

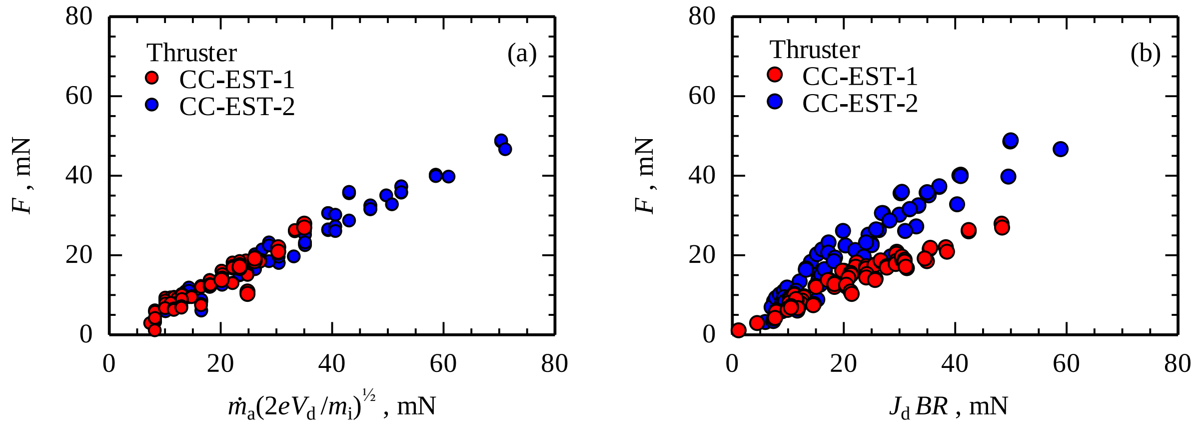

Figure 3 (a) electrostatic acceleration and (b) electromagnetic acceleration characteristics in CC-EST-1 and 2. Operating conditions are summarized in Table 1.

Table 2 Calculated thrust coefficients.

Thruster type	B, mT	α'	α	α_{EM}	α_{ES}
CC-EST-1	100	0.70	0.76	0.39	0.37
	150		0.69		0.3
	200		0.61		0.22
	250		0.55		0.16
CC-EST-2	210	0.69	1.18	0.64	0.54
	315		0.99		0.35
	402		0.92		0.28

The calculated α values depended on B (as summarized in Table 2). The α decreased as increasing B. CC-EST-2 showed higher α than that of CC-EST-2. Table 2 also summarized α_{EM} and α_{ES} values. In both thrusters, α_{EM} and α_{ES} were comparative. Hence, both electrostatic and electromagnetic acceleration contributed to generate thrust. Within the experimental conditions investigated in this study, the maximum thrust density was 39 N/m^2 and 52 N/m^2 for CC-EST-1 and CC-EST-2, respectively. Compared to conventional electrostatic thrusters, CC-ESTs have higher thrust density than that of cylindrical Hall thruster[7] (22 N/m^2), HEMP thruster[8] (37 N/m^2), cusped field thruster[9] (15 N/m^2), and comparable with state-of-the-art Hall thruster[10] SPT-140 (50 N/m^2). This high thrust density capability due to the electrostatic-magnetic hybrid plasma acceleration should be further improved in further studies.

IV. Conclusion

In this study, we developed the two types of CC-ESTs (CC-EST-1 and CC-EST-2). Two thrusters showed similar thrust characteristics that the obtained thrust were well fit to both the electrostatic thrust and electromagnetic thrust regardless of operating conditions. Calculated thrust coefficients for the electrostatic thrust and electromagnetic thrust were comparable. However, CC-EST-2 showed higher thrust coefficient than that of CC-EST-1. These tendencies indicate that both electrostatic and electromagnetic plasma accelerations contribute to generating thrust, namely the electrostatic-magnetic hybrid thrust generation was demonstrated. Because of the hybrid plasma acceleration method, thrust density reached 50 N/m^2, which is comparable or even higher with respect to conventional electrostatic thrusters.

Acknowledgments

This research was supported by the Japan Society for Promotion of Science, Grants-in-Aid for Scientific Research (A) No. 18H03813 and for Young Scientists No. 18K13925. The authors thank A. Saito at the Technical Division, Nagoya University, for their valuable technical assistance.

References

[1] Child, C. D., "Discharge from hot CaO," *Physical. Review.* (Series I), Vol. 32, No. 5, 1911, pp. 492–511.

[2] Dannenmayer, K., and Mazouffre, D., "Elementary Scaling Relations for Hall Effect Thrusters," *Journal of. Propulsion and Power*, Vol. 27, No. 1, 2011, pp. 236-245.

[3] Krulle, G., Kurtz, A., M., and Sasoh, A., "Technology and Application Aspects of Applied Field Magnetoplasmadynamic Propulsion," *Journal of. Propulsion and Power,* Vol. 14, No. 5, 1998, pp. 754-763.

[4] Sasoh, A., Kasuga, H., Nakagawa, Y., Matsuba, T., Ichihara, D., and Iwakawa, A., "Electrostatic-magnetic-hybrid thrust generation in central-cathode electrostatic thruster (CC-EST)," *Acta Astronautica*, Vol. 152, 2018, pp. 137-145.

[5] Ichihara, D., and Sasoh, A., "Similar Thrust Performance in Diverging-Magnetic-Field Electrostatic Thruster with Monoatomic Propellants," *Journal of Propulsion and Power*, Vol. 35, No. 1, 2019, pp. 236-238.

[6] chihara, D., Uno, T., Kataoka, H., Jeong, J., Iwakawa, A., and Sasoh, A., "Ten-Ampere-Level, Applied-Field-Dominant Operation in Magnetoplasmadynamic Thrusters," *Journal of Propulsion and Power*, Vol. 33, No. 2, 2017, pp. 360-369.

[7] Smimov, A., Raitses, Y., and Fisch, N. J., "Parametric Investigation of Miniaturized Cylindrical and Annular Hall Thrusters," *Journal of Applied Physics*, Vol. 92, No. 5, 2002, pp. 5673-5679.

[8] Koch, N., Harmann, H. P., and Komfeld, G., "Status of THALES High Efficiency Multi Stage Plasma Thruster Development for HEMP-T 3050 and HEMP-T 30250," *Proceedings of the 30th International Electric Propulsion Conference,* IEPC Paper 2007-110, Electric Rocket Propulsion Soc., Florence, 2007.

[9] Hu., P., Liu, H., Gao, Y., Mao, W., and Yu, D., "An Experimental Study of the Effect of Magnet Length on the Performance of a Multi-Cusped Field Thruster," *Journal of Physics D: Applied Physics*, Vol. 49, No. 28, 2016, Paper 285201.

[10] Goebel, D., M., and Katz, I., *Fundamentals of Electric Propulsion: Ion and Hall Thrusters,* A John Wiley and Sons, Inc., Hoboken, New Jersey, 2008.